

# STUDIES ON SMR SSI RESPONSES UNDER NONVERTICALLY PROPAGATING SEISMIC WAVES FOR NONUNIFORM SOILS WITH ABRUPT VARIATIONS OF STIFFNESS WITH DEPTH

Dan M. Ghiocel

President, Ghiocel Predictive Technologies, Inc., New York (dan.ghiocel@ghiocel-tech.com)

## ABSTRACT

The paper investigates the effects of inclined seismic waves on the deeply embedded SMR structures founded on nonuniform soils with abrupt stiffness variations with depth. Earlier preliminary studies on deeply embedded structures indicated that for uniform soils, the seismic wave inclined incidence effects are practically negligible, while for nonuniform soils with abrupt stiffness variations with depth, these effects can become significant. For highly nonuniform soils with abrupt soil stiffness variations, inclined incidence body wave scattering could produce high-order mode Rayleigh waves with low-decay rates which may have visible effects in high frequencies. These surface waves could amplify SMR structure responses in both horizontal and vertical directions. Specifically, the paper focuses on the effects of inclined incidence SV and SH waves. The paper includes results of several SSI studies using SMR structure FE models with different refinement levels. These SSI case studies include 3D detailed SMR structure model under inclined SV and SH waves for two selected stiff soil sites typical to Eastern US zone, but also simplified 2D and 3D SMR structure models under inclined body waves for different nonuniform soil deposits with either horizontal or oblique soil layering. The paper provides insights for understanding the effects of nonvertically seismic waves on deeply embedded SMR designs.

## INCLINED SEISMIC WAVES

The nonvertically propagating plane-waves include inclined SV, SH and P body waves, and Rayleigh and Love surface waves. The paper focus is on seismic plane-waves that produce horizontal soil motions in the excitation direction, specifically on the effects of the inclined SV and SH waves in highly nonuniform soils for which high-order Rayleigh waves may occur in the scattered wave mix.

When the control point is selected at the outcrop of the bedrock, the amplification of the soil motion to the free surface of the site depends on the angle of incidence of the incoming body waves. The amplification of the horizontal motion for incident SV-waves is affected strongly by the angle of incidence, being larger or smaller than for the vertical incidence (Wolf and Oberhuber, 1982). But, this is not the case for the soil amplification of the motion caused by SH-waves for which the more the wave propagation deviates from the vertical incidence, the more the amplification decreases over the entire frequency range (Luco and Wong, 1997).

For uniform soils, the surface waves attenuate much faster than the S and P body waves, especially in the higher frequency. However, this might be true for nonuniform soils with abrupt stiffness variation with depth. For highly nonuniform soils, higher-order mode Rayleigh surface waves may occur at higher frequencies. The higher-order mode Rayleigh waves have a completely different variation with depth than the first mode Rayleigh wave.

Four decades earlier, Seed and Lysmer in their valuable SSMRP Phase I report to LLNL stated (Seed and Lysmer, 1980): *“While most of these (Rayleigh) higher modes can be neglected, since they decay rapidly in the direction of propagation, others may decay less rapidly than the fundamental mode. This phenomenon occurs only at relatively high frequency on sites with a marked increase in stiffness with depth; say a sand profile over rock.”* ... *“There is in fact evidence to suggest that most of the energy approaching the ground surface results from body waves inclined within about 30 degree of the vertical. These includes the effects of the high-order surface wave modes.”*

## SMR CASE STUDIES

This section presents a summary of results of several studies which are grouped in two major SSI cases:  
 1) Detailed SMR SSI model under inclined SV and SH waves for two sites typical for Eastern US and  
 2) Simplified SMR model under inclined S and P waves for a nonuniform horizontally layered soil site and an obliquely layered soil site. All SMR SSI studies were performed with the ACS SASSI software (GP Technologies, 2022)

### Case 1: Detailed 3D SMR Structure Model Under Inclined SV and SH Waves

A description of the deeply embedded SMR SSI and structure FE models are shown in Figure 1. The SMR structure is a RC structure with a horizontal section size of 100ft by 100ft, and a total vertical size of 162.50 ft including an embedment of 118 ft and a super-structure height above ground of 44.50 ft. The SMR SSI FE model has a total of 30,924 nodes with 15,780 nodes used for excavated soil. The excavated soil model includes 29 embedment layers, plus 2 bottom soil layers used to ensure a transition to a regular mesh for excavation per the USNRC/BNL102434-2013 report recommendations (Nie et al., 2013). For the SSI analyses, the Fast FV (FFV w/skip 2) method was applied, with 7,491 interaction nodes corresponding to the excavation volume outer nodes plus 11 internal node layers. The FFV method is a refined ESM described in the ASCE 4-16 standard, with the interaction nodes defined for excavation outer nodes plus several internal layer nodes (Ghiocel, 2014, GP Technologies, 2022).

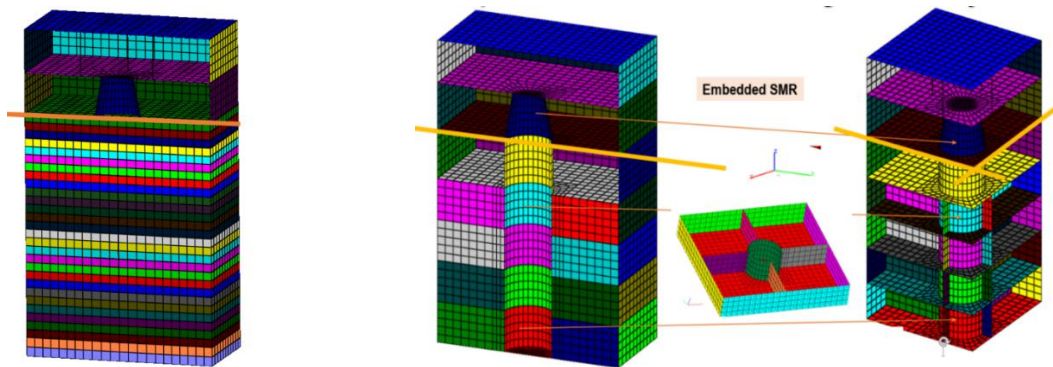


Figure 1 Description of ACS SASSI Embedded SMR SSI Model (left) and Structure Model (right)

Two generic soil profiles typical for the Eastern US sites were considered for the Case 1 study. The  $V_s$  profiles are illustrated in Figure 2 (left): 1) *Site 1* (red), a soil profile with a gradual stiffness increase down to a hard bedrock with  $V_s = 9,500$  fps at 1,100 ft depth, and 2) *Site 2* (blue) a soil profile having two abrupt stiffness variations at 80 ft depth (above SMR foundation depth) to a soft rock formation and at 300 ft depth to a hard rock formation, down to a hard bedrock with  $V_s = 9,200$  fps at 1,100 ft depth.

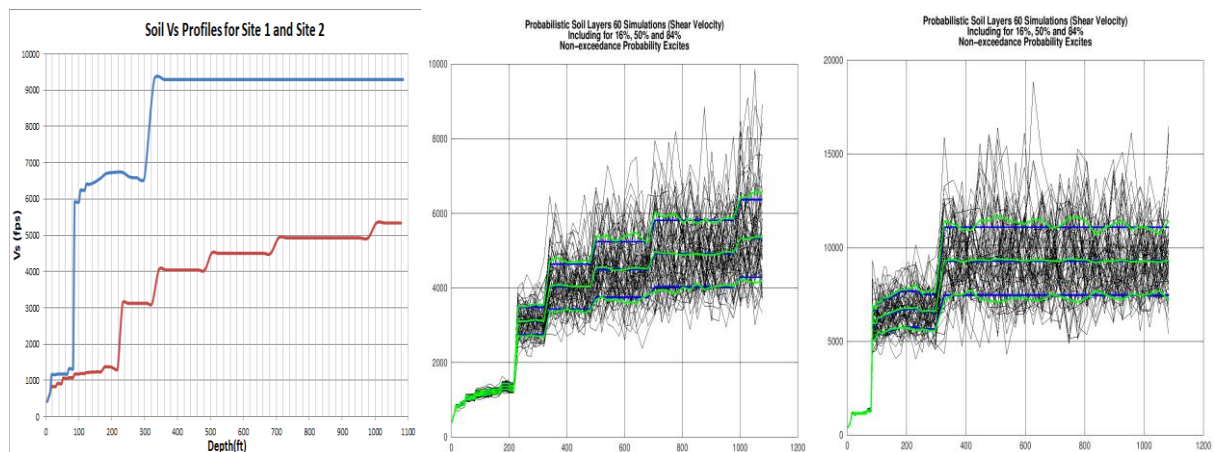


Figure 2 BE  $V_s$  Profiles for Sites 1 and 2 (left); Simulated  $V_s$  Profiles for Sites 1 (mid) and 2 (right)

To determine the seismic GMRS in horizontal direction at the SMR foundation level, 60 probabilistic simulated soil profiles (Figure 2 mid, right) and bedrock UHRS spectrum-compatible input acceleration motions were simulated using the ACS SASSI Option PRO per the ASCE 4-16 Sections 2 and 5.5 recommendations. Figure 3 shows the 60 probabilistic bedrock UHRS which are anchored at 0.20g ground acceleration. It should be noted that for the two generic soil profiles, the GMRS calculation procedure deviates from the probabilistic site response methodology accepted by NRC regulators for site-specific applications, since a simple UHRS randomization was applied, instead of the bedrock UHRS deaggregation procedure per RG 1.208. This simple procedure was accepted for the sake of simplicity for this research study. Separate UHRS input motion simulations were performed for X and Y directions. Same bedrock UHRS inputs were defined for Sites 1 and 2.

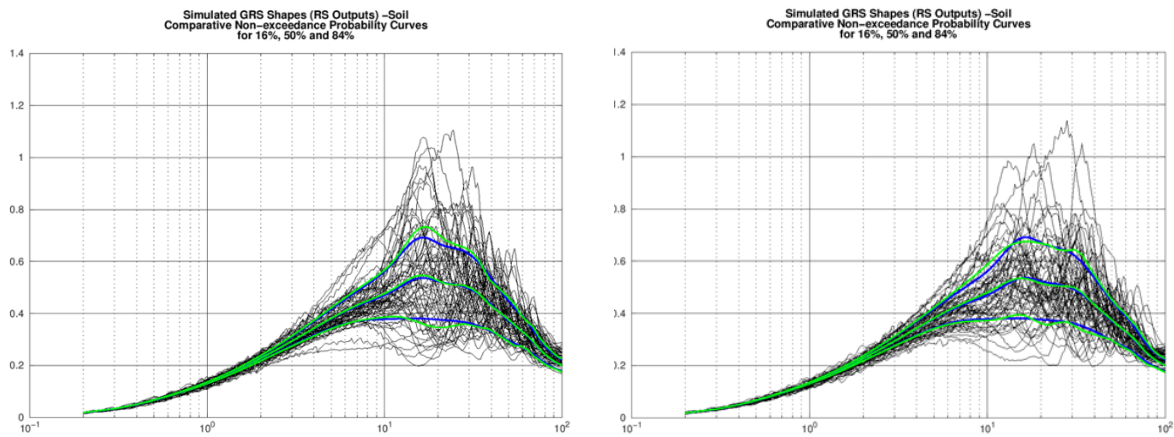


Figure 3 Probabilistic Simulations of Bedrock UHRS Inputs; X-Direction (left) and Y-Direction (right)

The probabilistic site response was performed assuming vertically and nonvertically propagating SV and SH waves for each of the two sites. The nonvertically SV and SH waves were considered having a 20 degrees inclination angle from the vertical direction. The SV waves were input for X direction plane and the SH waves were input for Y direction plane. No seismic wave incidence angles were defined horizontal plane deviating from X and Y axes.

Using the ACS SASSI code, the 60 GRS motions were computed for all depth levels of interest. Figures 4 and 5 show for Site 1 and Site 2, based on the 60 probabilistic site response simulations, the Mean and the 80 NEP in-column GRS computed at the SMR foundation at 118 ft depth. It should be noted that the SV wave motion amplitude for 20 degrees angle incidence has a much larger scatter than for vertical incidence.

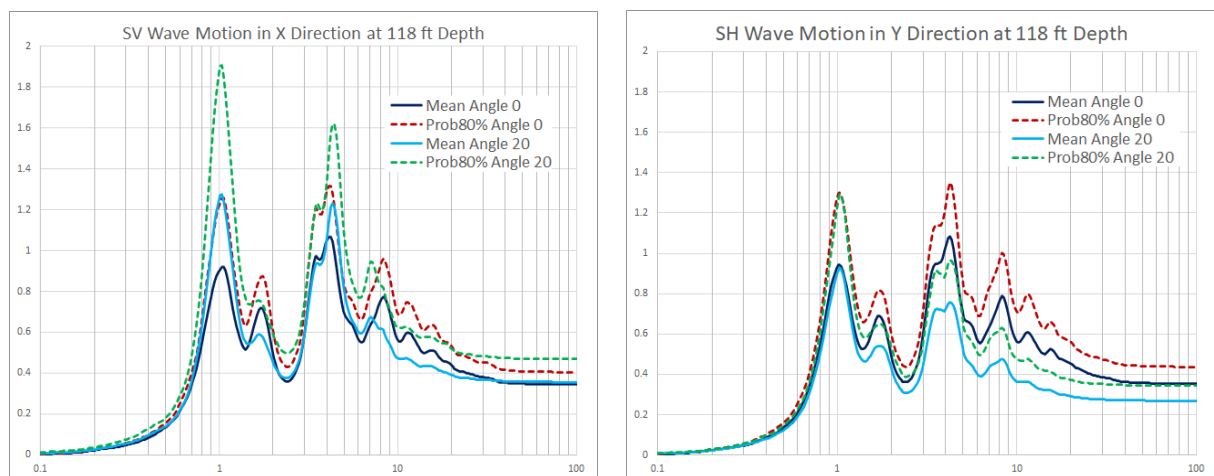


Figure 4 Site 1 Free-Field GRS in X and Y Directions at the SMR Foundation Level (El. -118 ft)

As expected, for X direction, the SV wave soil motion amplifications for the 20 degree incidence angle are both above and below the SV motion amplifications for vertical incidence, while for Y direction, the

SH wave soil motion amplifications for the 20 degree incidence angle are for all frequencies below the SH motion amplifications for vertical incidence.

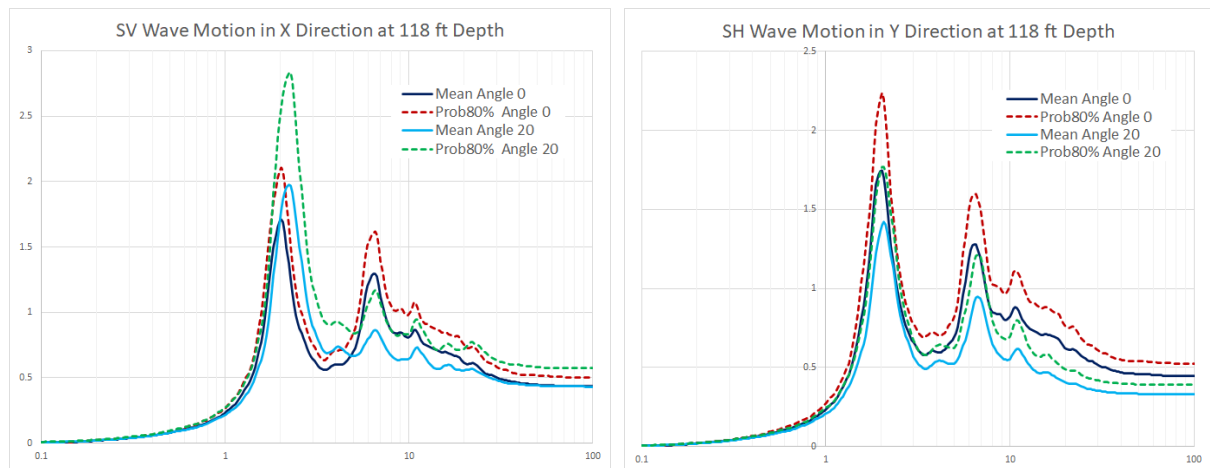


Figure 5 Site 2 Free-Field GRS in X and Y Directions at the SMR Foundation Level (El. -118 ft)

Further, deterministic SSI analyses were performed using the Mean and 80% NEP computed GRS as seismic inputs at the SMR foundation (El. -118ft) and assuming the BE soil profiles shown in Figure 2.

A total of eight cases were performed in this study for the two sites with two seismic GRS input levels and two angles of incidence. The SV and SH wave inputs were input simultaneously for SSI analysis in X direction and Y direction, respectively. Figures 6 and 7 show for Site 1 the horizontal ISRS computed within the SMR structure for two corner locations at elevation - 30ft (below ground surface) and elevation 44.5 ft (at roof).

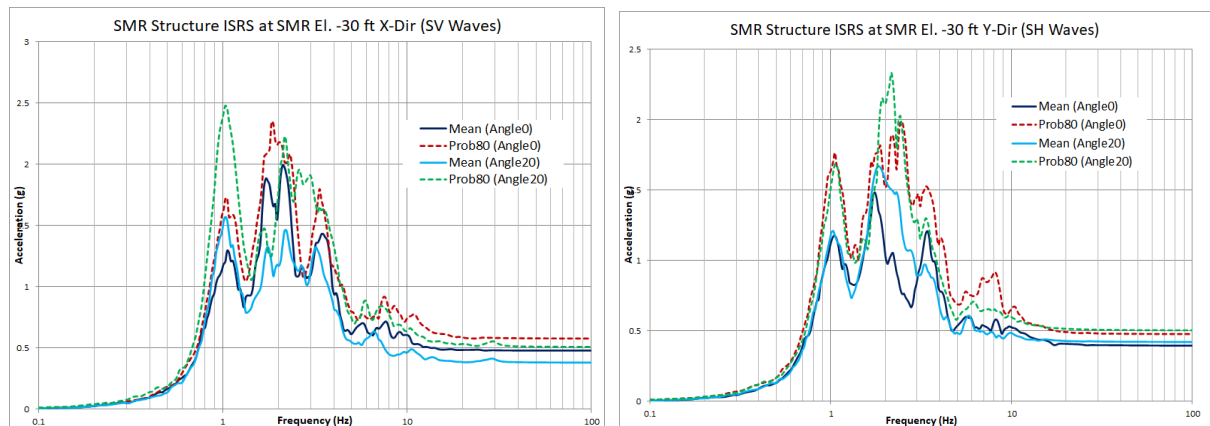


Figure 6 Site 1 SMR ISRS in X and Y Directions below Ground Surface Level (El. -30 ft)

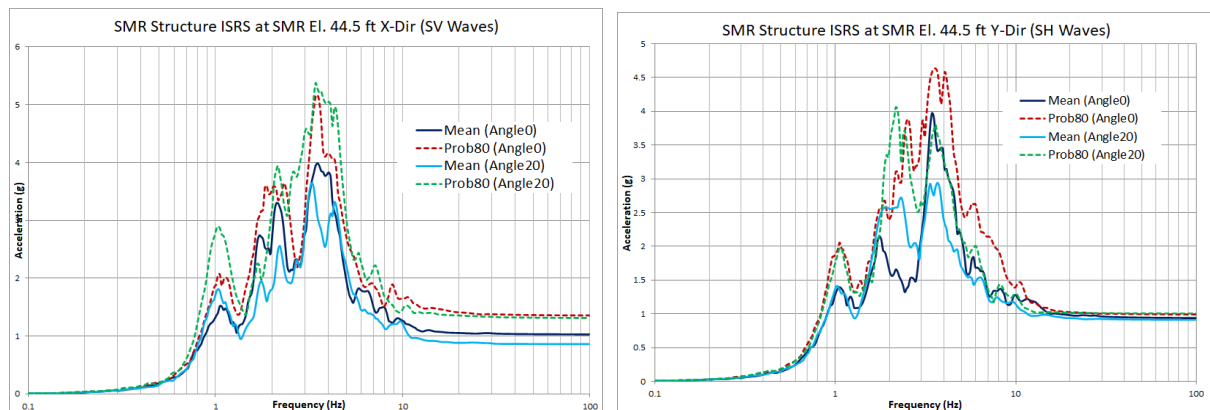


Figure 7 Site 1 SMR ISRS in X and Y Directions at Top of Structure (El. 44.50 ft)

Figures 8 and 9 show for Site 2 the horizontal ISRS computed within the SMR structure for the same locations used in Figures 6 and 7 for Site 1.

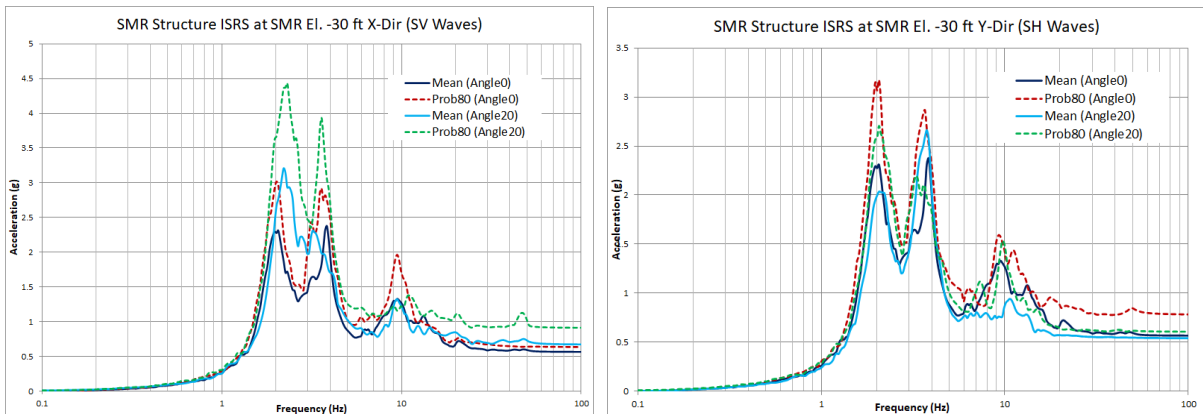


Figure 8 Site 2 SMR ISRS in X and Y Directions below Ground Surface Level (El. -30 ft)

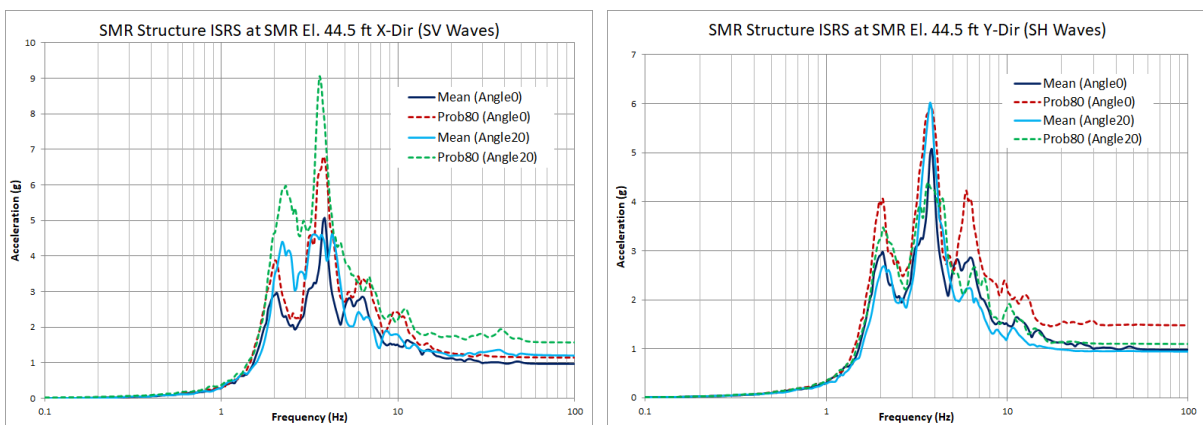


Figure 9 Site 2 SMR ISRS in X and Y Directions at Top of Structure (El. 44.50 ft)

ISRS in Figures 6 and 7 indicate that for Site 1 in X direction the SV waves produced 25-30% larger ISRS amplitudes for the lowest frequency peak @ 1.1 Hz and lower ISRS amplitudes for other frequencies, while the SH waves produced 15-20% larger ISRS amplitudes for the peak @ 1.8 Hz.

ISRS in Figures 8 and 9 indicate that for Site 2, the SV waves produced 35-40% larger ISRS amplitudes for the lowest frequency peak @ 2.2 Hz and lower ISRS amplitudes for other frequencies, while the SH waves produced 15-20% larger ISRS amplitudes for the amplification peak @ 3.8 Hz.

As expected based on the USNRS regulatory requirements for the deeply embedded SMR structures, the SSI computed ISRS results shown in the above figures indicate that the effects of nonvertically propagating SV and SH waves could be significant, well above the 10% variation acceptability level.

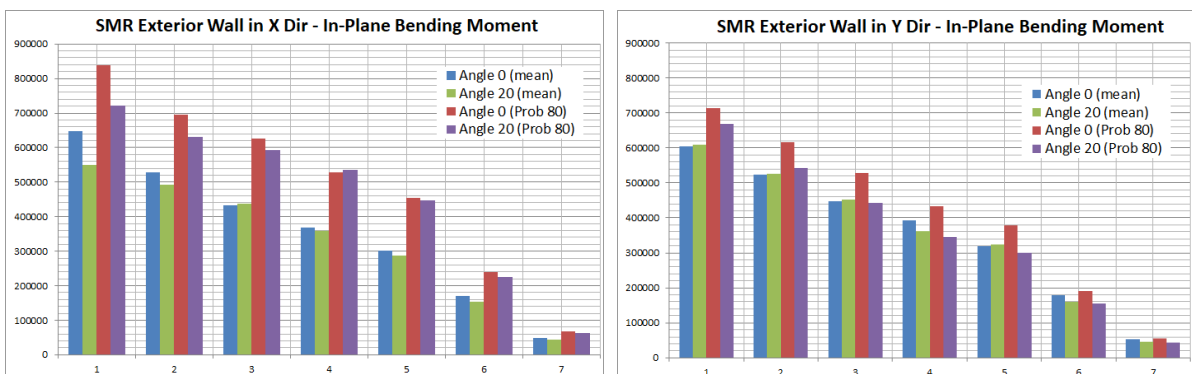


Figure 10 Site 1 Bending Moments in SMR Exterior Walls (for 7 Floor Levels) in X and Y Directions



Figure 11 Site 2 Bending Moments in SMR Exterior Walls (for 7 Floor Levels) in X and Y Directions

Figures 10 and 11 show the computed in-plane bending moments in the SMR exterior RC wall for Site 1 and Site 2, respectively. These figures show much less differences in results for vertical and inclined incidence, mostly less than 10%, except for the SV waves for Site 2, for which differences can go for some floor levels up to about 20% for Mean GRS inputs, and up to 35% for 80% NEP GRS inputs.

**Case 2: Simplified SMR Structure Under Inclined SV and SH Waves**

*Case 2A: 3D SMR SSI Model with A 100ft Shallow Soil Layer Above Bedrock*

A simplified deeply embedded 3D SMR SSI model considered. The SMR structure is a RC structure with a horizontal section size of 100ft by 100ft, and a total vertical size of 200 ft with an embedment of 140 ft and a super-structure height above ground of 60 ft. The SMR SSI FE model shown in Figure 12 has a total of 3,756 nodes. The SMR excavation model includes 14 embedment layers. Both structure and excavation models have a regular FE mesh. For an investigated case including abrupt soil stiffness variation, SSSI effects were also considered, as shown in Figure 13.

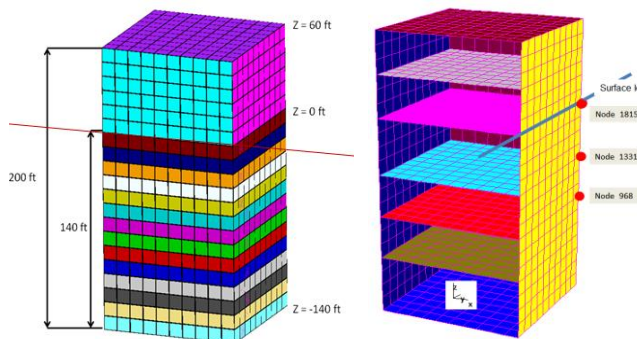


Figure 12 Simplified SMR SSI Model

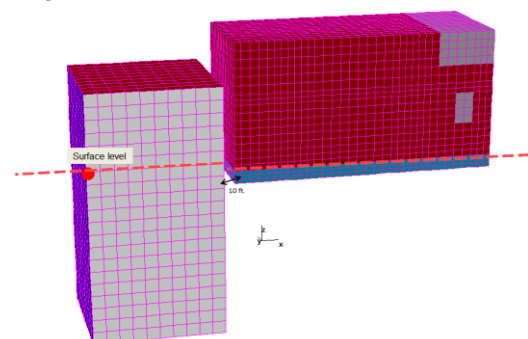


Figure 13 Simplified SMR-AB SSSI Model

The horizontally layered soil deposit consists of a shallow 100ft depth soil layer with  $V_s = 2,500$ fps above a rock formation with  $V_s = 6,000$ fps (Figure 14).

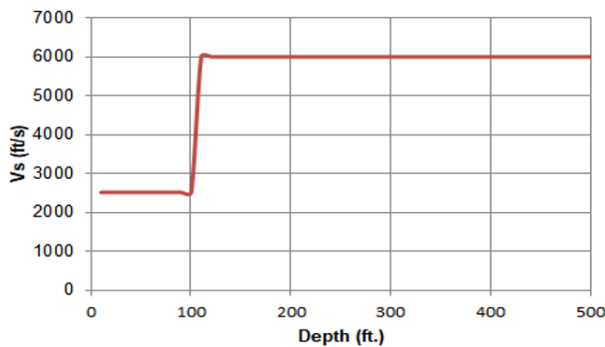


Figure 14 Highly Nonlinear Soil Profile

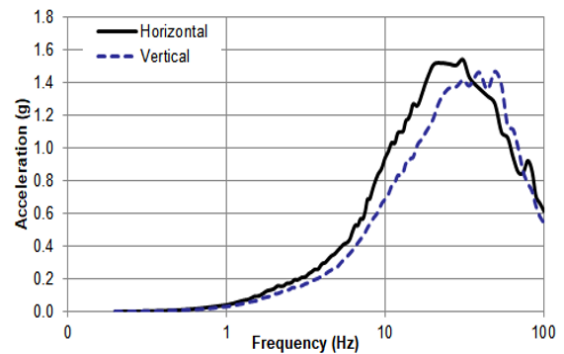


Figure 15 Bedrock UHRS Seismic Input

The 140ft embedment SMR is embedded in the rock formation. The seismic excitation is defined by a high-frequency outcrop UHRS input with a ground acceleration of 0.30g at the bedrock depth of 500 ft. (Figure 15). The seismic input at bedrock is a HRHF spectra with a high spectral amplification up to 1.5g (largest for Eastern US sites).

In addition to the standalone SMR SSI model, a SMR SSSI model is also considered. The SSSI model includes the deeply embedded SMR structure and a neighboring the shallowly embedded AB structure at a 10 ft distance. Seismic inputs consisted of vertically and nonvertically propagating SV, SH and P waves with a 10 degrees incidence angle. The ISRS computed for the vertically and nonvertically incidence waves for the standalone SMR SSI model (solid line) and the SSSI SMR-AB model (dashed line) are shown in Figures 16 and 17. The ISRS are computed at the SMR structure corners. Figure 16 shows the SMR horizontal ISRS in X-direction at an elevation below the ground surface and at the ground surface level, respectively. Figure 17 shows the vertical ISRS at the same elevation below the ground surface and at the top of structure, respectively.

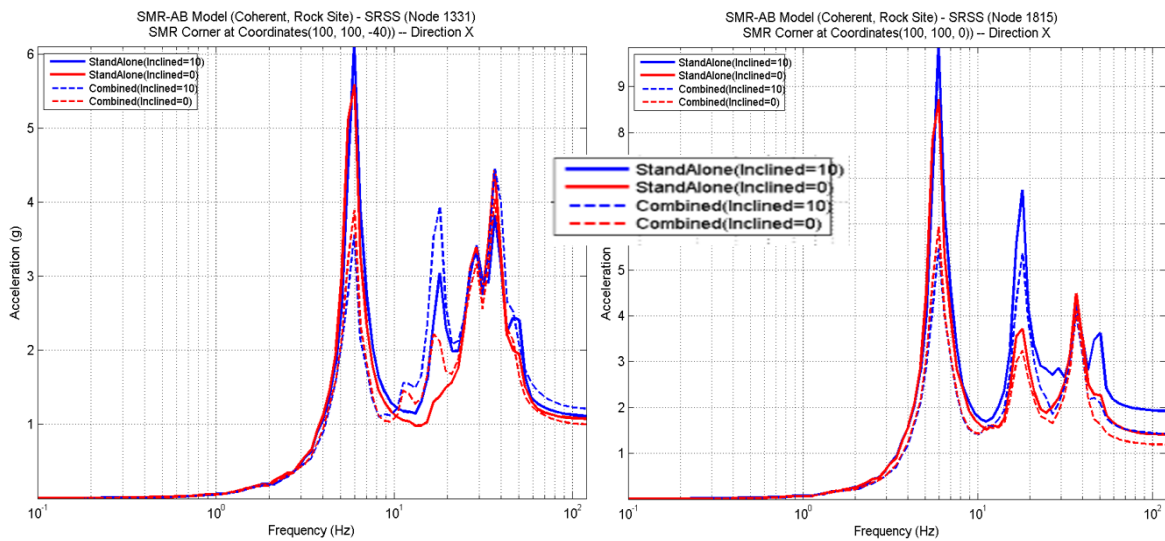


Figure 16 Horizontal ISRS Below Ground (El. – 40ft) and Surface Levels (El. 0ft) X-Direction

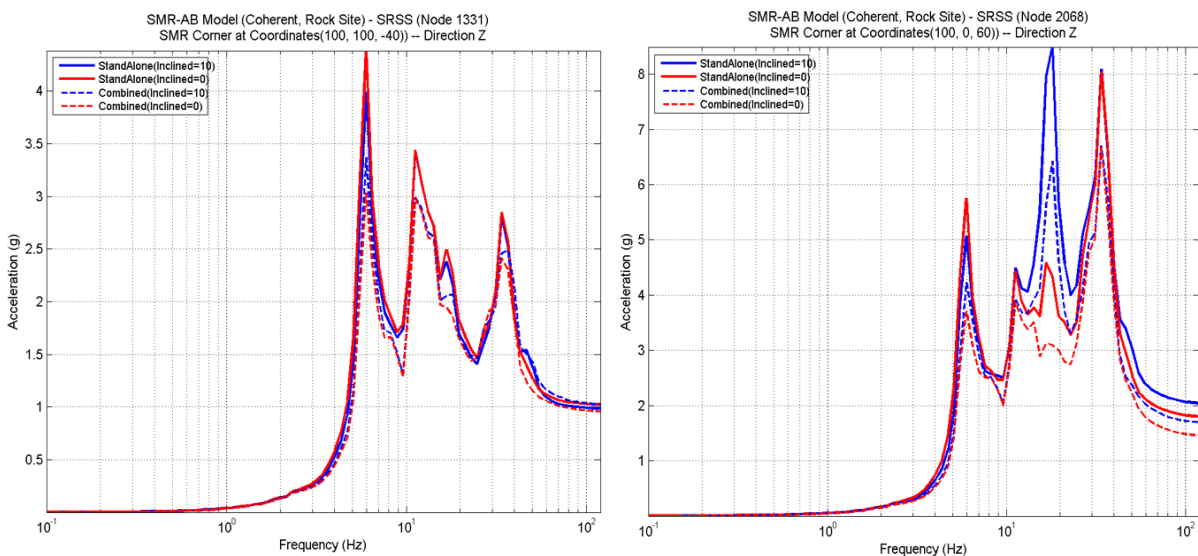


Figure 17 Vertical ISRS Below Ground (El. – 40ft) and Top of Structure (El. 60ft) Z-Direction

Large amplifications are noted for the ISRS peak @ 18 Hz due for the inclined wave input. The ISRS spectral peak @18 Hz frequency is highly amplified up to 100% in both the horizontal and vertical directions due to the seismic wave inclined incidence. However, this amplification is not visible in the vertical direction at the SMR corner at the -40 ft elevation below ground surface. This indicates that this

18 Hz frequency peak amplification is a likely to be a result of an increased ground surface motion under a significant presence of a higher-order mode Rayleigh wave component with a frequency close to the 18 Hz frequency. The SSSI effects also may increase ISRS amplitudes for inclined seismic waves.

It should be noted the same SMR SSI model was also analyzed under vertically and nonvertically propagating waves for an uniform soil with  $V_s = 1,500$  fps. No visible ISRS amplifications were observed for this case due to the inclined seismic wave effects.

*Case 2B: 2D SMR SSI Model with Nonuniform Soil Layer Sites*

To further clarify the noted issues, a sensitivity study was done for a 2D simplified SSI model for the same SMR structure. Two soil profiles were considered: 1) *Site 1*, with a nonuniform soil, with a gradual increase of the soil stiffness with depth, with  $V_s$  gradually varying from 1,750 fps to 4,000 fps at 200 ft depth and below, going down to the hard bedrock at 800 ft depth (Figure 18), and 2) *Site 2*, with a nonuniform soil, with an abrupt variation of the soil stiffness on 100 ft depth, with a shallow soil layer with  $V_s = 2,500$  fps and a thickness of 100 ft above a rock formation with  $V_s=6,000$  fps going down to a hard bedrock at 800 ft depth. The *Site 2* soil layering is similar with the previous Case 1A site soil layering for the simplified 3D SMR structure model (Figure 14), with the difference of the hard bedrock that is at 800 ft depth instead of 500 ft depth as in previous study. The seismic input for Site 1 and Site 2 applied at the bedrock at 800 ft depth is shown in Figure 19.

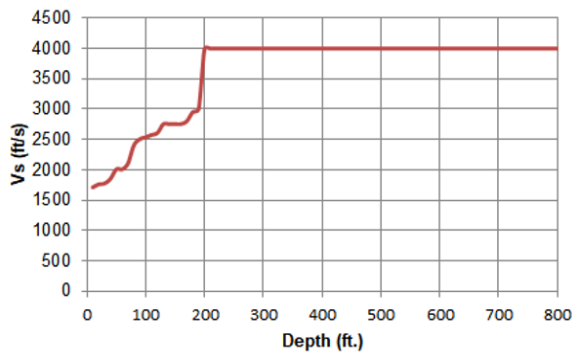


Figure 18 Nonlinear Soil Profile

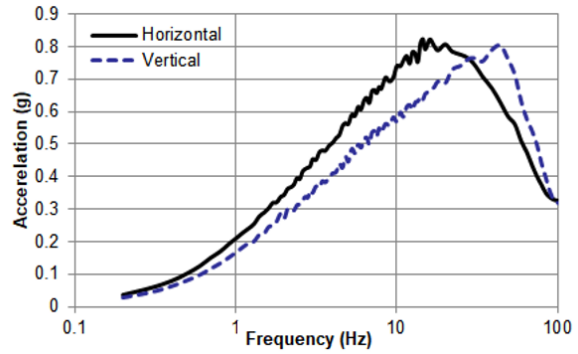


Figure 19 Bedrock UHRS Seismic Input

The seismic 2D SMR SSI analyses were performed for vertically and nonvertically SV-P waves. The wave incidence angle was parametrically varied for 0, 10 and 30 degree angles with the vertical direction. Comparative ISRS computed at the top corner of the SMR structure in X and Z direction are shown in Figures 20.

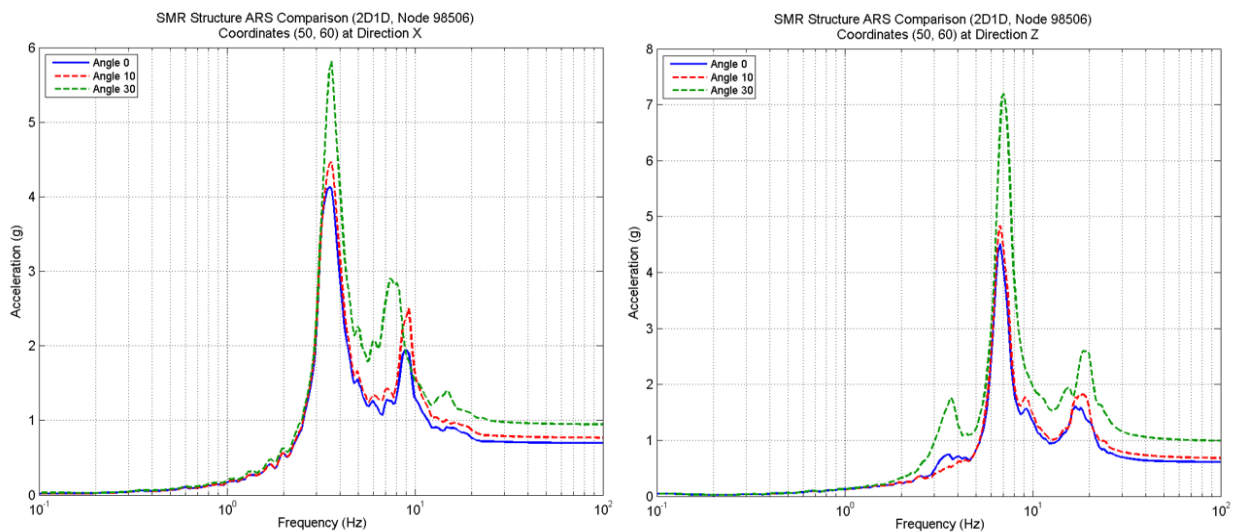


Figure 20 The Effects of SV-P Wave Incidence Angle on SMR Structure ISRS; 0 Degree Angle (blue line), 10 Degrees Angle (red line) and 30 Degrees Angle (green line)

Computed ISRS indicate that for Site 1, the 10 degree incidence angle effects on SSI response are quite minor, while the 30 degree incidence angle effects are significant, up to a 40-45% ISRS peak increase. Then, the SSI analyses were repeated for the Site 2 soil profile for 10 degree incidence angle. Computed ISRS are shown in Figure 21.

It should be noted that the 10 degree incidence angle has a reduced effect by less than 10% increase for Site 1 with gradual soil stiffness increase with depth, and a large effect by up to 50% increase for Site 2 with abrupt soil stiffness increase with depth.

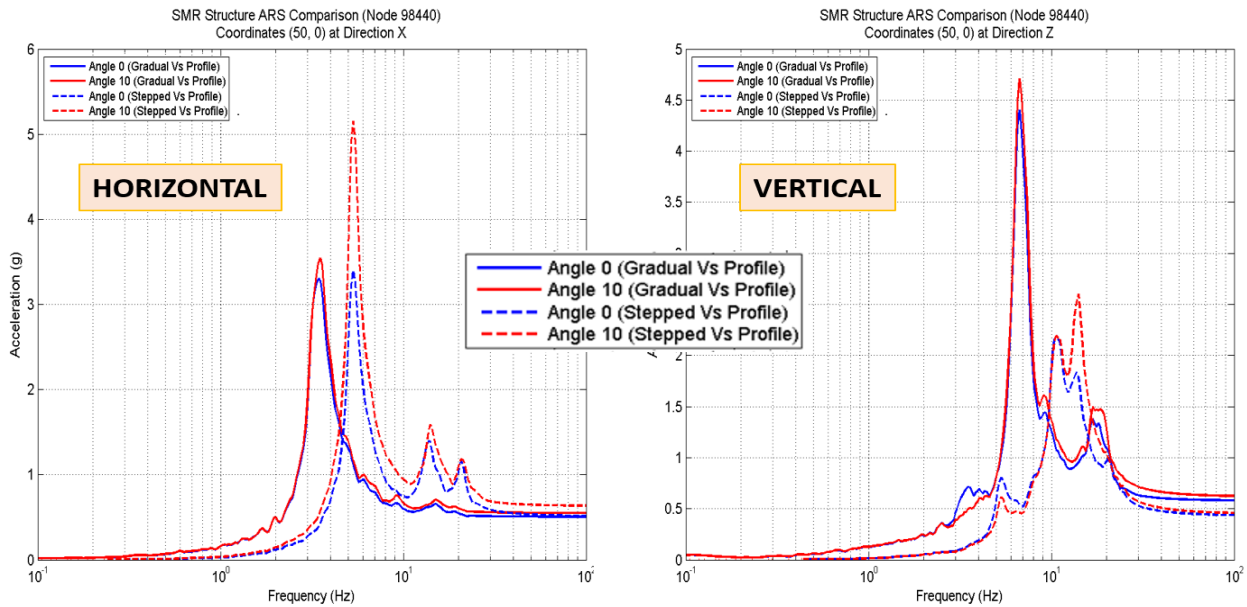


Figure 21 The Effects of Seismic Wave Incidence on SMR ISRS at Ground Surface Elevation Level Computed for 0 and 10 Degree Incidence Angle for Site 1 and Site 2

For Site 2, the 10 degree incidence angle produced large effects of on ISRS (Figure 21), which are quite similar to the SSI results computed using the 3D SMR model for Case 2A (Figure 16). The ISRS peak amplifications at @ 6Hz and 18 Hz is present in both Figures 16 and 21. However, due to the significantly higher amplitude seismic input in the high frequencies for the Case 2A, the 18 Hz ISRS peak amplification is much larger in Figure 16 than Figure 21, while the 6 Hz ISRS peak amplification is lower in Figure 16 and Figure 21. Differences in the ISRS amplifications are also due to the larger SSI radiation damping for the 2D SMR case than for 3D SMR case.

*Case 2C: 3D SMR SSI Model with Nonuniform Soil Inclined Layering*

The simplified 3D SMR structure model and a truncated part of the inclined soil layering with a 6,000 ft horizontal size and a 200 ft depth size (shown at a distorted space scale) are shown in Figure 22. The lateral extension of the FE mesh is 16,000 ft to avoid any artificial boundary effects on the wave propagating. The layered soil includes layers with a Vs varying from 1,500 fps to 4,000 fps, as shown in Figure 22. It should be noted that the average Vs values for the 2D soil model for a horizontal space window of 500 ft size in vicinity of SMR foundation has the same values with the Vs values provided for the *Site 1* horizontally layered soil model shown in Figure 18.

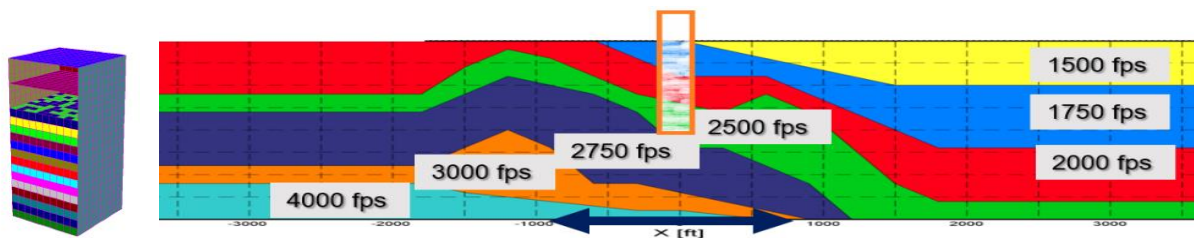


Figure 22 Simplified 3D SMR Structure and 2D Soil Profile Model with Inclined Layers

The seismic input was defined in the horizontal direction only at the bedrock using the same UHRS as in Figure 19, assuming a wave vertical incidence. The inclined waves are produced by the wave scattering due to the inclined soil layering with slopes up to 1:10 in the vicinity of the SMR foundation. The SSI analysis was performed using an “enhanced” SASSI methodology for which the excavated soil impedance and free-field motion are based on a 2D soil model (3D2D SSI modeling; 3D structure with 2D soil layering) rather than a 1D soil model (3D1D SSI modeling; 3D structure with 1D soil layering) as in the “standard” SASSI methodology. The 3D2D SSI modeling is described elsewhere (Ghiocel, 2019) and was implemented in the ACS SASSI Option 2DSOIL software (GP Technologies, 2019).

Figure 23 shows the embedded SMR structure corner ISRS in the horizontal and vertical directions computed using the 3D2D model and 3D1D model, respectively, at the ground surface level (Node 1, upper plots) and the top of structure (Node 1695, mid plots) elevations. For comparison the acceleration transfer function (ATF) amplitudes computed in free-field at the ground surface (lower plots). Two dominant SMR structure ISRS spectral peaks are noted @ 3.5 Hz and 9 Hz frequencies, and a minor peak @ 16 Hz. The effects of the inclined waves are visible for the 3.5 Hz and 9 Hz horizontal ISRS peaks at the top of SMR structure, and not much visible at the foundation level. It should be noted that the 3D2D model with inclined soil layers reduces the 3.5 Hz peak and amplifies the 9 Hz peak. This indicates that inclined waves significantly affect the SMR structure rocking motions associated with the 3.5 Hz and the 9 Hz frequency SSI vibration modes.

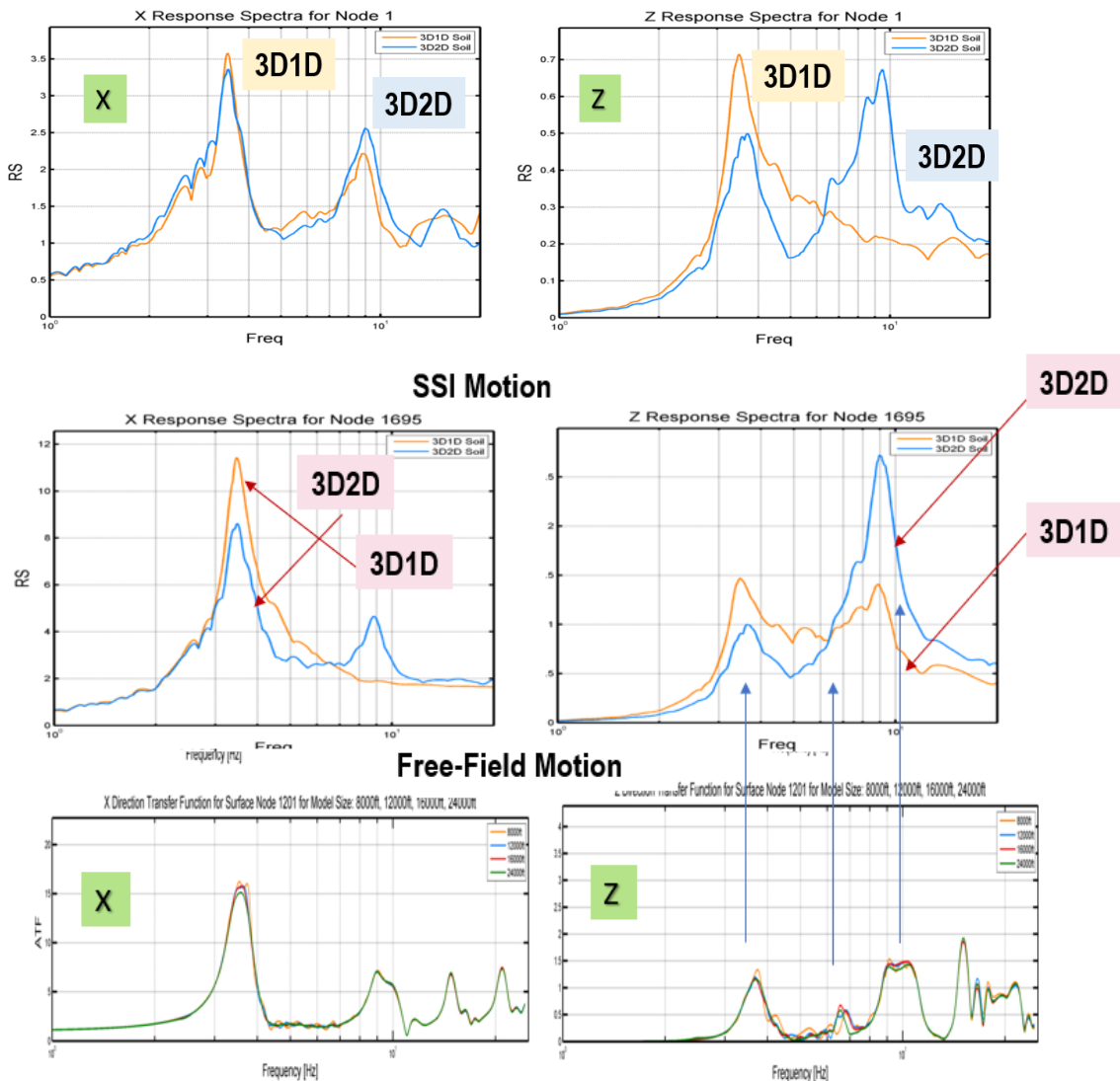


Figure 23 SMR ISRS at Ground Surface Level and Top of Structure (upper and middle plots), and ATF Amplitude for Free-Field Surface (lower plots) for X and Z Directions

It should be noted that these spectral peaks also correspond to the 3.5 Hz, 9 Hz and 18 Hz peaks in Figure 20, especially for the ISRS computed at the top of SMR structure (please see ISRS plotted in Figure 20 left vs. Figure 23 mid-left). Apparently, the large ISRS amplification changes in Figure 23 due to the inclined seismic wave effects indicate a better matching for the ISRS computed for the 30 degrees incidence angle shown in Figure 20. This result is also partially influenced by the soil impedances that are different for the horizontally layered soil and the obliquely layered soil. It should be noted that since the 2D SMR SSI model has a significantly larger SSI radiation damping than the 3D SMR SSI model, the ISRS peak values are reduced for the 2D SMR SSI model (Figure 20) in comparison with the 3D SMR SSI model (Figure 23).

## CONCLUDING REMARKS

The paper presents a summary of results from several SSI studies on the effects of the inclined seismic waves on deeply embedded SMR structures. The investigated SMR case study results, confirmed that the inclined wave effects in nonuniform soil deposits can be significant on computed ISRS but less significant on structural forces and moments.

The inclined seismic wave effects are notably larger for nonuniform soils with abrupt stiffness variations at shallow depths than for nonuniform soils with gradual stiffness variations with depth. For nonuniform soils with abrupt stiffness variations at a shallow depth, the presence of the higher-order mode Rayleigh wave components with low-decay rates can amplify sensibly the ISRS spectral peaks in the mid and high frequencies for both horizontal and vertical directions as discussed herein.

## REFERENCES

- American Society of Civil Engineers (2017), *Seismic Analysis for Safety-Related Nuclear Structures and Commentary*, ASCE 4-16 Standard
- GP Technologies, Inc. (2022). *ACS SASSI Version 4.3 User Manual, Including Advanced Options A-AA, NON, PRO, RVT-SIM and UPLIFT*, Revision 7, Pittsford, New York, January 31.
- GP Technologies, Inc. (2019). *ACS SASSI Option 2DSOIL for Soil Deposits with Oblique Layering*, Technical Internal Reports and User Guide, Rev 0, Pittsford, New York
- Ghiocel, D.M. (2014). *SASSI Methodology-Based Sensitivity Studies for Deeply Embedded Structures, Such As Small Modular Reactors (SMRs)*, U.S. Department of Energy Natural Phenomena Hazards Meeting, Germantown, MD, October 21-22
- Ghiocel, D.M. (2019). *Extending SASSI Methodology to Seismic SSI Analysis for NPP Buildings on Soil Deposits with Inclined Waves*, SMiRT25, Division III, Charlotte, NC, August 4-9
- Luco, J.E. and Wong, H.L. (1979). *Response of Structures to Nonvertically Incident Seismic Waves*, Univ. of California at San Diego, Report, Dept. of Applied Mech. And Eng. Sciences
- Nie, J., Braverman, J., and Costantino, M. (2013). *Seismic Soil-Structure Interaction Analyses of A Deeply Embedded Model Reactor – SASSI Analyses*, U.S. Department of Energy, Brookhaven National Laboratory, BNL 102434-2013, New York
- Seed, B.H. and Lysmer, J. (1980). *The Seismic Soil-Structure Interaction Problem for Nuclear Facilities*, Seismic Safety Margin Research Program, SSMRP Phase I report to LLNL, CA
- Wolf, J.P. and Oberhuber, P. (1982). *Free-Field Response from Inclined SV- and P-Waves and Rayleigh Waves*, Journal of Earthquake Engineering & Structural Dynamics, Vol 10, 847- 869